The Reaction of Peroxy Radicals with OH Radicals

Christa Fittschen

Université Lille, CNRS, UMR 8522 - PC2A - Physicochimie des Processus de Combustion et de l'Atmosphère, F-59000 Lille, France

Tel: +33 3 20 33 72 66, e-mail Christa.fittschen@univ-lille.fr

Revised version

Submitted to

Chemical Physics Letters

March 21, 2019

Abstract

The reaction of peroxy radicals, RO_2, with OH radicals has long been ignored to play any role in atmospheric chemistry. Recent experimental and modeling studies show however that these reactions are fast and can play a role in remote atmospheres with low NO concentrations when the major fate of peroxy radicals, its reaction with NO, slows down. The present article summarizes recent work on this class of reactions and its implications in different environments.

Introduction

Peroxy radicals, RO_2, are key species in atmospheric and low temperature combustion chemistry. They are reactive intermediates formed during the oxidation of most hydrocarbons:

$$RH + OH \rightarrow R + H_2O \quad (R1)$$

$$R + O_2 \rightarrow RO_2 \quad (R2)$$

In the atmosphere, their subsequent reaction depends on the environment. A detailed review on their chemistry has been given by G. Tyndall and collegues [1,[2]. Briefly, in polluted environments, *i.e.* in the presence of high NO_x concentrations, peroxy radicals will rapidly react with NO to form NO_2 and alkoxy radicals, RO.

$$RO_2 + NO \rightarrow RO + NO_2 \quad (R3)$$

The NO_2 will be photolysed and leads to an increase in O_3 concentration.

$$NO_2 + h\nu \rightarrow NO + O(^3p) \xrightarrow{O_2} O_3 \quad (R4)$$

The alkoxy radicals react further with O_2, leading to a carbonyl species and HO_2, which oxidizes another NO to NO_2 and finally leads to formation of a second O_3 molecule:

$$RO + O_2 \rightarrow R_{-H}O + HO_2 \quad (R5)$$

$$HO_2 + NO \rightarrow OH + NO_2 \quad (R6)$$

With decreasing NO concentration, other reaction pathways become competitive for peroxy radicals. Until recently, only the reactions with HO_2 or the self- and cross reactions with other peroxy radicals, leading mostly to stable products, were considered as fate for RO_2 radicals under low NO conditions in atmospheric chemistry models such as MCM [3,[4,[5]. For the simplest RO_2, CH_3O_2, this leads to:

$$CH_3O_2 + HO_2 \rightarrow CH_3OOH + O_2 \quad (R7)$$

$$CH_3O_2 + CH_3O_2 \rightarrow 2\ CH_3O + O_2 \xrightarrow{O_2} CH_2O + HO_2 \quad (R8a)$$

$$CH_3O_2 + CH_3O_2 \rightarrow CH_3OH + CH_2O + O_2 \quad (R8b)$$

In 2009, Archibald *et al*. [6] proposed for the first time an alternative reaction pathway for RO_2 in low NO environments: the reaction of RO_2 radicals with OH radicals. In a pure modeling study they investigated the possible impact of this class of reaction on the composition of the atmosphere. They simulated the impact of such a reaction in the Marine Boundary Layer (MBL) by adding to their mechanism the reaction of OH with peroxy radicals up to C_4 and compare the concentrations with the

base case, *i.e.* without RO_2 + OH. Three different possible reaction paths were simulated, leading for the example of the most simple peroxy radical, CH_3O_2, to the following products:

$$OH + CH_3O_2 \rightarrow CH_2O_2 + H_2O \quad \text{(R9a)}$$

$$OH + CH_3O_2 \rightarrow CH_3O + HO_2 \quad \text{(R9b)}$$

$$OH + CH_3O_2 \rightarrow CH_3OH + O_2 \quad \text{(R9c)}$$

They run the three different product scenarios by varying the rate constants for all RO_2 + OH reactions between 0.5, 1.0 and 1.5×10^{-10} cm^3s^{-1}. For all scenarios they found only a small, negligible effect on the mixing ratios of O_3, NO_x, OH, and other trace gas species in the marine boundary layer. However, a substantial increase in the mixing ratios of HCOOH was observed for all simulated rate constant scenarios, if the reaction pathway would be formation of the Criegee radical (R9a). A strong increase in the mixing ratio of CH_3OH was observed if the major pathway would be (R9c). The impact on the RO_2 and HO_2 radical budget was very minor for all scenarios.

Even though this study pointed towards a possible, non-negligible impact of this class of reaction on the composition of remote atmospheres, no further attention was paid to this reaction in the following years and it was only in 2014 that Bossolasco *et al*. [7] measured for the first time the rate constant of a reaction between a peroxy radical and an OH radical. The rate constant turned out to be fast enough to make this reaction non-negligible under remote environments and since then, several aspects of this class of reaction have been studied experimentally and theoretically by different research groups.

In the following article, a résumé of the findings on the reaction of RO_2 radicals with OH radicals and the impact of this class of reactions on the composition of the atmosphere in different environments will be summarized. The article is separated in two parts: the reaction of the most simple peroxy radicals, CH_3O_2, with OH radicals will be discussed separately in the first part, and the reaction of larger RO_2 radicals with OH will be discussed in the second part. Each section will first discuss the current knowledge on the rate constants and in a second subsection summarizes what is known about the product yields and what impact this reaction might have on the composition of the troposphere.

The reaction of CH_3O_2 + OH

Rate constant

The first measurement of a rate constant for the reaction of a peroxy radical with OH radicals was reported in 2014 by Bossolasco *et al.* [7]. Using laser photolysis coupled to cw-cavity ring down spectroscopy for a quantification of CH_3O_2 [8] and high repetition rate LIF for a time resolved detection of OH radicals [9] they investigated the reaction of the simplest peroxy radical

$$CH_3O_2 + OH \rightarrow \text{ products} \quad \text{(R9)}$$

The schematic view of the experimental set-up used for most of the studies so fare published on RO_2 + OH reactions is shown Figure 1.

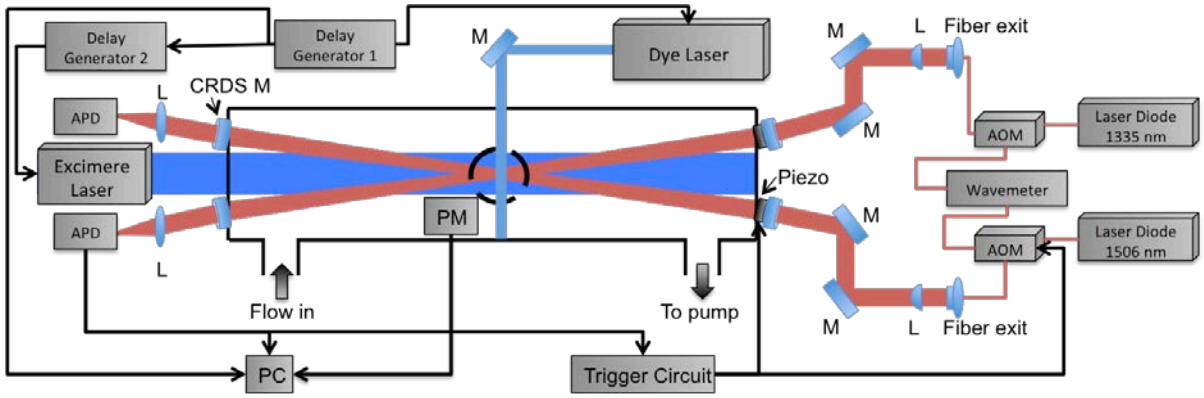

Figure 1: Schematic view of experimental set-up: excimer laser generates simultaneously OH and RO_2 radicals from appropriate precursors, 2 symmetric cw-CRDS paths for detection of absolute, time resolved traces of HO_2, CH_3O_2 or OH cross the photolysis pulse in a small angle, leading to an overlap of 37 cm between photolysis and detection beam, high repetition rate laser induced fluorescence for detection of relative OH concentration time profiles is installed perpendicular to the photolysis beam. APD: Avalanche Photo Diode, AOM: Acousto-Optic Modulator, M: Mirror, L: Lens, PM: photomultiplier. Separate, identical trigger circuits and data acquisition systems are used for both cw-CRDS systems, but are not shown in the figure for clarity.

The 248nm photolysis of CH_3I in the presence of O_2 was used as a precursor for CH_3O_2 radicals, while OH radicals were simultaneously generated by photolysis of H_2O_2 [10]. Using this method, they found a very fast rate constants of $k_9 = (2.8\pm1.4)\times10^{-10}$ cm^3s^{-1}. With such a fast rate constant, this reaction could indeed become competitive to the other reaction paths. CH_3O_2 is an important radical, particularly over the tropical oceans where, in absence of other hydrocarbons emitted by flora or human activity, OH radicals process a large fraction of the global CH_4 emission. Neglecting an important reaction path for this radical might therefore lead to a bias in HO_x concentration, CH_4 lifetime or O_3 formation and destruction rate. Fittschen *et al.* [11] have integrated (R9) into the detailed MCM model [4] and have determined the importance of (R9) as a sink of CH_3O_2 radicals in remote marine environments. Conditions such as found during a field campaign at Cape Verde Island [12] in 2007, representative for the tropical remote ocean, were simulated using the rate constant from Bossolasco *et al*. [7] and it has been shown that up to 30% of all CH_3O_2 radicals would decay through (R9). Following the work of Bossolasco *et al*., Yan *et al*. [13] have re-measured the rate constant of the reaction of OH radicals with CH_3O_2 using laser photolysis coupled to UV-absorption spectroscopy, radicals were generated by simultaneous 193nm photolysis of CH_3COCH_3 as precursor for CH_3O_2 radicals and N_2O/H_2O as precursor for OH. The absorption-time profiles were fitted to a complex mechanism containing 46 reactions, with many of them being radical-radical reactions. A rate constant of $k_9 = (8.7\pm1.7)\times10^{-11}$ cm^3s^{-1} at 298K was obtained, more than a factor of 3 slower than Bossolasco *et al*. In order to elucidate such a large difference, Assaf *et al*. [14] have measured again the rate constant of (R9) using the same set-up as Bossolasco *et al*. [7]. In this work, the photolysis of XeF_2 in the

presence of CH_4 and H_2O was used to simultaneously generate CH_3O_2 and OH radicals instead of the co-photolysis of CH_3I/H_2O_2. A rate constant of $k_9 = (1.6\pm0.4)\times10^{-10}$ cm^3s^{-1} was obtained, nearly a factor of 2 slower than the earlier determination by the same group [7], but still nearly a factor of 2 higher compared to the result of Yan *et al*. [13]. The high rate constant of Bossolasco *et al*. is now thought of having been induced by the presence of I-atoms (or accumulated I_2 molecules) when using CH_3I as precursor for CH_3O_2 radicals: a follow-up study of the reaction of larger peroxy radicals with OH radicals [15] showed the same behavior, *i.e*. a much faster rate constants when using the corresponding alkyl-iodides as precursor for the peroxy radicals (for more details see below). However, the rather large difference between the results of Assaf *et al*. [14] and Yan *et al*. [13] could not be explained. The measurements of Assaf *et al*. [14] are in principle more direct, *i.e.* less secondary reactions take place in their system, compared to the measurements of Yan *et al*. The rate constants obtained in both studies rely directly on the absorption cross sections of CH_3O_2 radicals used to transform the absorption time profiles into absolute CH_3O_2 concentration and any error in the absorption cross section would directly translate into a proportional error in the rate constant. Yan *et al*. used UV-absorption spectroscopy, a wavelength region where the absorption cross sections of peroxy radicals are well studied and believed to be well-known, while Assaf *et al*. used cw-CRDS in the near IR-region, a wavelength range much less explored. Indeed, the absorption cross section of CH_3O_2 in the near IR region is still discussed controversially: the value such as determined by Farago *et al*. [8] ($\sigma_{7489.16\ cm^{-1}} = (3.4\pm0.4)\times10^{-20}$ cm^2) and used by Assaf *et al*. is 2 to 3 times higher than the only two other determinations of this absorption cross sections that were published at that time [16,[17]. A too large absorption cross section would return a too small CH_3O_2 concentration and thus a too high rate constant. Even though Farago *et al*. produced possible reasons for the differences in their absorption cross sections compared to literature values (disregard of diffusion by Atkinson an Spillman [17] and disregard of secondary reactions by Pushkarsky *et al*. [16]), the doubt persisted. In 2016, Assaf *et al*. [14] re-determined the CH_3O_2 absorption cross section using not by using the kinetic method, i.e. measuring the CH_3O_2 decay and taking advantage of the known rate constant to retrieve the initial CH_3O_2 concentration, but relative to the cross section of HO_2 radicals, which is believed to be well known [18,[19,[20,[21]: they photolysed XeF_2 in the presence of either CH_3OH/O_2 or CH_4/O_2, and generated this way either HO_2 or CH_3O_2. Assuming on the basis of the known chemistry the near-complete conversion of F-atoms into either HO_2 radicals or CH_3O_2 radicals, the absorption cross section is then measured relative to the well-know HO_2 value, and the initially obtained value by Farago *et al*. [8] was confirmed. However, in 2018 Assaf *et al*. have carried out a detailed investigation of the reaction system of F + CH_3OH [22] and they were able to determine experimentally for the first time the rate constant of the reaction

$$CH_3O + HO_2 \rightarrow \text{products} \qquad \text{(R10)}$$

The rate constant was found to be very fast (k_{10} = 1.1×10^{-10} cm^{3}s^{-1}), in contrary to the only available estimations [23,[24] that predicted rate constants orders of magnitude slower (10^{-13} cm^{3}s^{-1}). With such a fast rate constant, the reaction of CH_3O+HO_2 is not anymore negligible under the condition of the re-determination of the absorption cross section of CH_3O_2 by Assaf *et al.* in 2016. The same is true for the CH_3O self-reaction:

$$CH_3O + CH_3O \rightarrow \text{products} \qquad \text{(R11)}$$

The rate constant had been estimated by Tsang and Hampson [24] to lead to the formation of CH_2O and CH_3OH with a very fast rate constant of k_{11}=1×10^{-10} cm^{3}s^{-1} while the few experimental determinations [25,[26,[27,[28,[29,[30] obtained lower values between (1.1–3.8) ×10^{-11} cm^{3}s^{-1}, mostly from fitting reaction systems to complex mechanisms. Assaf *et al*. [22] determined k_{11}=7×10^{-11} cm^{3}s^{-1}, making this reaction also significant under their conditions. **Figure 2** shows a re-evaluation of the experimental data from Figure 3 in Assaf *et al*. [14] that had been used to re-determine the absorption cross section of CH_3O_2: the magenta line shows the model of the HO_2 profile without (R10) and (R11) and leads to an initial F-atom concentration of 4.4×10^{12}cm^{-3}, converting the initial CH_3O_2 absorption coefficient (red symbols) into σ= 3.4×10^{-20} cm^2. The black line show the model including (R10) (F-atom concentration converted to products of this reaction as dashed green line in **Figure 2**) and (R11) (F-atom concentration converted to products of this reaction as dashed blue line in **Figure 2**), now yielding an initial F-atom concentration of 6.8×10^{12}cm^{-3}. This higher initial F-atom concentration results in a proportionally lower absorption cross section for CH_3O_2: σ = 2.2×10^{-20} cm^2.

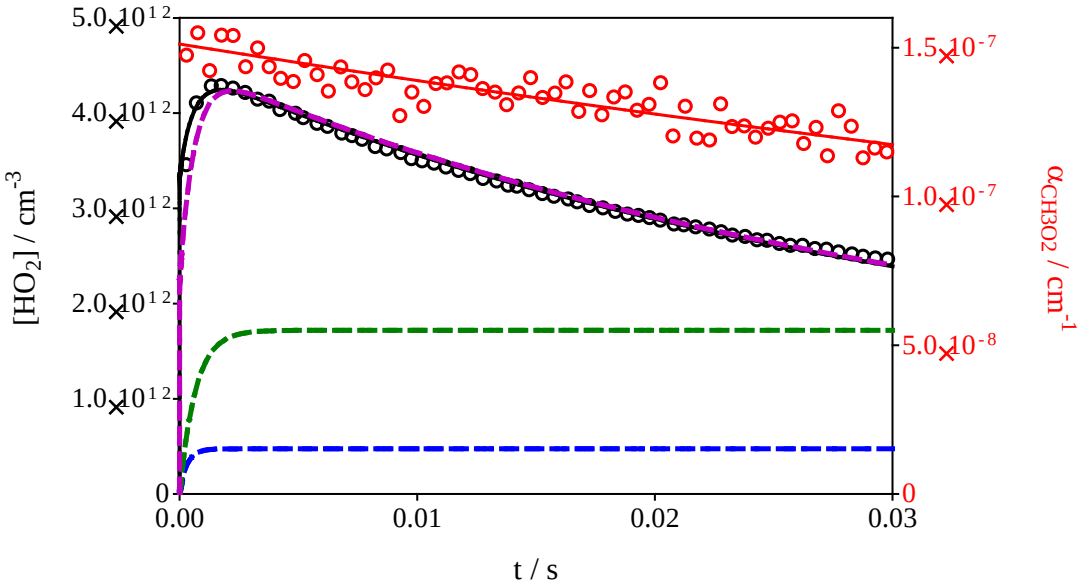

Figure 2: Data from Figure 3 in Assaf *et al*. 2016 [14]. Concentration time profile of HO_2 (black symbols, left y-axis) and absorption coefficient of CH_3O_2 (red symbols, right y-axis) as a function of time. 248nm photolysis of XeF_2 was the radical source, and experiments have been carried out back-to-back by using either 2.8×10^{15} cm^{-3} CH_3OH / 4.7×10^{17} cm^{-3} O_2 to generate HO_2 or 8.5×10^{15} cm^{-3} CH_4 / 4.7×10^{17} cm^{-3} O_2 to generate CH_3O_2. H_2O concentration was below 3×10^{14} cm^{-3}, OH was below

detection limit. Full black line corresponds to a model taken from Assaf *et al.* 2018 [22], dashed magenta line presents the model neglecting (R10) and (R11).

This value is in good agreement with a very recent determination by Onel *et al.* [31], who finds 1.49×10^{-20} cm^2 at 7487.98 cm^{-1}, translating to 1.9×10^{-20} cm^2 at the wavelength used by Assaf *et al.* (7489.16 cm^{-1}). Assaf *et al.* had also applied the kinetic method to their experiments using XeF_2 as precursor (black symbols in **Figure 3**). Even though the initial radical concentrations using XeF_2 were much lower than for the experiments Farago *et al.* using CH_3I (red symbols in **Figure 3**), and with this the uncertainty of the extrapolation of the linear regression to $I = 0$ (black line in **Figure 3**, giving $m_{I=0} = (2.9\pm0.4)\times10^7$ cm s^{-1}) was higher (*i.e.* the loss of CH_3O_2 due to diffusion was much more important than for Farago *et al.* : red line in **Figure 3** with $m_{I=0} = (2.8\pm0.2)\times10^7$ cm s^{-1}), this method also confirmed the absorption cross section in agreement with the value of Farago *et al.*. The blue line in **Figure 3** represents a regression with the intercept forced to a value (4.36×10^7 cm s^{-1}, dotted line in **Figure 3**) corresponding to $\sigma = 2.2\times10^{-20}$ cm^2. It can be seen that all decays from Assaf *et al.* are above the intercept corresponding to $\sigma = 2.2\times10^{-20}$ cm^2, *i.e.* in agreement with a decay through CH_3O_2 self-reaction plus an increasing loss through diffusion with decreasing concentration, while this is not true for Farago *et al*: all decays are *slower* than would be expected for CH_3O_2 decay only, and they become even slower with increasing concentration. This disagreement with the work of Farago *et al.* is currently not understood, maybe I-atom chemistry somehow perturb the CH_3O_2 decay [32,[33].

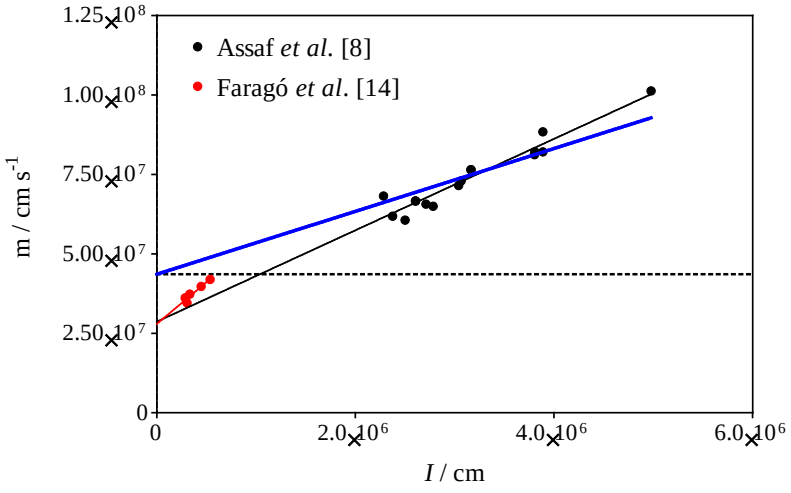

Figure 3: Data from Farago *et al* [8] (red symbols) and from Assaf *et al.* [14] (black symbols). Black line corresponds to a linear regression of the values of Assaf *et al.*, blue line is a regression forced to an intercept corresponding to $\sigma = 2.2\times10^{-20}$ cm^2.

Because the rate constant of (R9) such as determined by Assaf *et al.* (and Bossolasco *et al.*) directly depends on the absorption cross section of CH_3O_2, this now lower value entails a proportionally lower value of the rate constant: 1.0×10^{-10} cm^{3}s^{-1}. The new value is in good agreement with the value of Yan *et al.* [13] and it seems that near IR absorption cross section of CH_3O_2 and rate constant for (R9) are

settling towards a final value. This long story confirms the rule that rate constants decrease with time…. The results of the three experimental studies as well as the re-evaluated rate constant from Assaf *et al*. [14] using the re-evaluated absorption cross section for CH_3O_2 are summarized in **Table 1**.

Table 1: Summary of rate constant measurements for the reaction of CH_3O_2 + OH radicals

Method	Rate constant / cm^3s^{-1}	Remark	Reference
248 nm Laser photolysis of CH_3I / H_2O_2, detection of CH_3O_2 by cw-CRDS, OH by LIF	$(2.8\pm1.4) \times 10^{-10}$	Rate constant relies on near IR absorption cross section of CH_3O_2, rate constant probably biased by I / I_2	Bossolasco *et al*. 2014 [7]
193 nm Laser photolysis of CH_3COCH_3 / N_2O, detection of CH_3O_2 and OH by UV absorption	$(8.4\pm1.7) \times 10^{-11}$	Profiles fitted to complex mechanism, high initial radical concentrations up to 10^{14} cm^{-3}	Yan *et al*. 2016 [13]
248 nm Laser photolysis of XeF_2 / CH_4 / H_2O, detection of CH_3O_2 by cw-CRDS, OH by LIF	$(1.6\pm0.4) \times 10^{-10}$	Rate constant relies on near IR absorption cross section of CH_3O_2 (3.4×10^{-20} cm^{-2})	Assaf *et al*. 2016 [14]
	$(1.0\pm0.4) \times 10^{-10}$	Rate constant using absorption cross section re-evaluated (2.2×10^{-20} cm^{-2})	This work

Product yields and atmospheric implications

Following the first measurement of the rate constant k_9 by Bossolasco *et al*. [7], Fittschen *et al.* [11], came to the conclusion, that this reaction is a non-negligible sink for CH_3O_2 radicals over tropical oceans with up to 30% of CH_3O_2 reacting through this pathway. Even though the rate constant of (R1) has been revised since then and it can be estimated that (R1) will be proportionally less important as sink for CH_3O_2 (i.e. around 10%), it becomes important to determine the reaction products in order to appreciate the impact of this reaction on the composition of the atmosphere. Müller *et al*. [34] have investigated this question by means of detailed theoretical calculations as well as by integrating this reaction with different product branching scenarios into a global model. By high level *ab-initio* calculations they characterized the triplet and singlet potential energy surfaces (PES) and deduced that the triplet entrances are negligible: the dominant initial product is the singlet trioxide intermediate, CH_3OOOH

$$OH + CH_3O_2 \rightarrow CH_3OOOH \qquad \text{(R9d)}$$

which can either be stabilized or rapidly converted to a pre-product complex (CH_3O…HOO). The coupling of the triplet and singlet surfaces via intersystem crossing can affect the product distribution and makes a prediction of product distributions through RRKM calculations less reliable. The singlet state undergoes rapid bond scission and yields the bimolecular products CH_3O + HO_2 (R9b) with a small contribution to the channel CH_3OH + $O_2(^1\Delta)$ (R9c), while the triplet surface mostly yields CH_3O + HO_2 (R9b) with small contribution to CH_3OH + O_2 ($^3\Sigma_g^-$). Formation of the Criegee intermediate through pathway (R9a) has been excluded, which had also been found experimentally by Yan *et al.*

[13] and later by Assaf *et al.* [35]. Müller *et al*. [34] proposed that this reaction might help resolving a strong missing source of methanol over tropical oceans [36]. From running different product branching scenarios in their global model, they deduced that, when using the rate constant of Bossolasco *et al*., a yield of up to 30% CH_3OH would be needed as product of (R9) to bring into agreement measurements and models, while their RRKM calculations predicted only a yield of 7% for CH_3OH. Besides, it is now clear that the rate constant k_9 from Bossolasco *et al*. is too high by a factor of 3, which leads to an even higher yield that would be necessary for bringing into agreement model and measurements. Ferracci *et al*. [37] have run a global model to investigate the impact of (R9) on the composition of the atmosphere, now using the revised rate constant from Assaf *et al*. [14]. They found that an unreasonably high yield of ϕ_{CH_3OH} = 0.8 would be needed to reconcile model and measurements.

A first experimental indication on possible product yields of (R9) was given by Yan *et al*. [13] who deduced from modeling their UV absorption-time profiles to a complex mechanism an upper limit of 5% for the formation of the Criegee intermediate (R9a). This upper limit was later confirmed by Assaf *et al*. [35] using broadband cavity enhanced absorption spectroscopy [38]. Assaf *et al*. [35] could by simultaneous measurement of absolute HO_2 [18]and OH [39] concentration-time profiles determine the HO_2 yield (R9b) at a total pressure of 50 Torr Helium to be ϕ_{HO_2} = 0.8±0.2. This yield was slightly revised in a later work [40] to ϕ_{HO_2} = 0.9±0.1 because it was found in the meantime, that (R10) and (R11) are fast and played some role in the reaction system of Assaf *et al*. [35]. This high HO_2-yield left little room for a large CH_3OH yield, in agreement with the predictions of Müller *et al.* [34]. A very recent work by Caravan *et al*. [41] was then intended to a direct determination of the CH_3OH yield. Three different experimental set-ups where used: a low pressure (30 Torr) or a high pressure (740 Torr) laser photolysis reactor, both coupled to time resolved VUV photoionization mass spectrometry [42] as well as an atmospheric simulation chamber coupled to a detection of reaction products by PTR-ToFMS. From simulation of the laser photolysis experiments, a yield of ϕ_{CH_3OH} = 9±5 % and 6±2 % was obtained from experiments in the low and high pressure reactor, respectively. Experiments in the high pressure reactor also found evidence for a non-negligible yield of the stabilized trioxide, CH_3OOOH (R9d), no signal however could be detected when using the low pressure reactor. This is in good agreement with the calculations of Müller *et al.* [34], who predicted a yield for the stabilization of ϕ_{CH_3OOOH} = 7 % at 760 Torr and ϕ_{CH_3OOOH} = 0.02 % at 30 Torr. The experiments in the atmospheric simulation chamber resulted in a markedly higher yield of ϕ_{CH_3OH} = 17±3 %, not in agreement with the laser photolysis experiment, even considering the reciprocal error bars, while no CH_3OOOH signal could be detected in the simulation chamber / PTR ToFMS experiments, even though carried out at 760 Torr. It was therefore speculated that the trioxide, CH_3OOOH, is detected by the PTR-ToFMS at the mass of CH_3OH, thus increasing the apparent CH_3OH yield. It could not be decided if the

CH_3OOOH decomposes into CH_5O^+ upon protonisation or if CH_3OOOH is already decomposing heterogeneously into CH_3OH, either on the Teflon walls of the simulation chamber or on the walls of the sampling tubes. This hypothesis brings into excellent agreement theoretical calculations, Teflon chamber and laser photolysis experiments, as the CH_3OH yield determined in the Teflon chamber corresponds to the predicted sum of CH_3OH and CH_3OOOH. This now experimentally confirmed low CH_3OH yield results in an even decreased concentration of CH_3OH due to the decreased concentration of CH_3O_2 radicals (from its reaction with OH), whose self-reaction is the major source of CH_3OH in the remote atmosphere.

Experiment and theory corroborate the formation of the trioxide, CH_3OOOH, from the reaction between CH_3O_2 and OH radicals. The atmospheric fate of this new species is therefore of interest. Anglada and Solé [43] have recently employed high level theoretical methods to investigate the oxidation of CH_3OOOH by OH radicals. They found that the reaction can proceed by abstraction of either the terminal hydrogen atom of OOOH group leading to formation of CH_3O, O_2 and H_2O, or of one of the hydrogen atoms of the CH_3 group producing H_2CO, HO_2 and H_2O. They found that the abstraction of the terminal hydrogen atom of the OOH group is with $k = 4.7\times10^{-11}$ cm^3s^{-1} about 22 times faster than the abstraction of a hydrogen atom of the CH_3 group ($k = 2.1\times10^{-12}$ cm^3s^{-1}). The lifetime of CH_3OOOH in the troposphere has been predicted to be about 3.9 hours at 275 K and decreasing to 0.2 hours at 310 K. Such a lifetime could be sufficient to allow accumulation of sizeable concentrations of CH_3OOOH under very low NO concentrations. **Figure 4** summarizes the current knowledge on the branching of reaction products for the reaction of CH_3O_2 + OH.

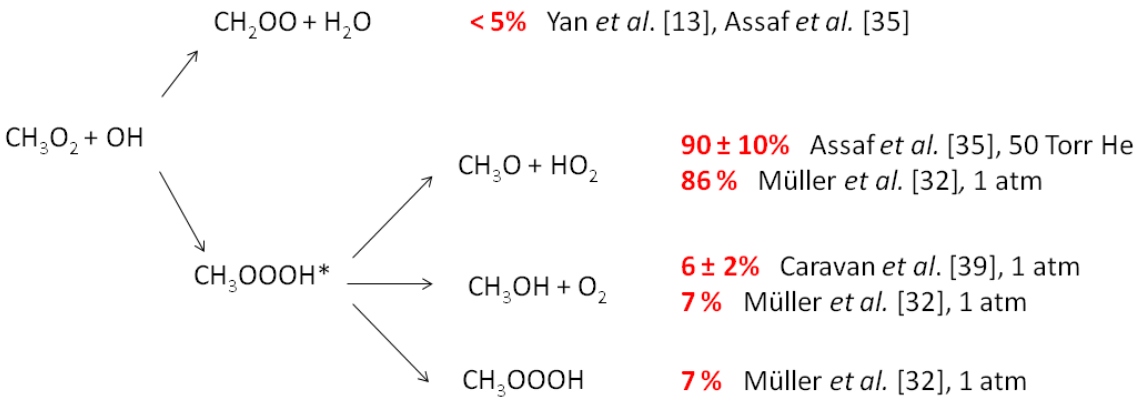

Figure 4: Summary of current knowledge on the reaction products for the reaction of CH_3O_2 + OH.

The reaction of larger RO_2 + OH

Rate constants

While the reaction of CH_3O_2 radicals with OH radicals plays an important role over remote tropical oceans, the reactions of larger peroxy radicals with OH could play a role in remote biogenic environments. Therefore, the rate constant of OH radicals with the next larger peroxy radical has been measured by Farago *et al*. [44]:

$$OH + C_2H_5O_2 \rightarrow \text{products} \qquad \text{(R12)}$$

In that work, OH radicals have been generated by photolysis of H_2O_2, i.e. the same way as in Bossolosco *et al*. [7], while the peroxy radicals were generated from the reaction of Cl-atoms (generated by simultaneous 248 nm photolysis of $(COCl)_2$) with C_2H_6. This method was not applicable for the generation of CH_3O_2: the reaction of CH_4 with Cl-atoms is only 16 times faster than the reaction of OH radicals with CH_4, while this ratio is around 250 in the case of C_2H_6. Therefore, the CH_4 concentrations necessary for rapidly converting Cl-atoms into CH_3 radicals would at the same time result in a fast reaction of OH radicals with CH_4 (and thus only a small fraction of OH radicals would react with CH_3O_2). Another difference between the two studies of CH_3O_2 radicals [7,[14] and the $C_2H_5O_2$ study was the quantification method of the absolute peroxy radical concentrations: in the case of CH_3O_2, the radicals were directly quantified by cw-CRDS absorption spectroscopy, and thus the rate constant directly relies on the absorption cross section of CH_3O_2 used to transform the absorption-time profiles into concentration-time profiles (see first part of this paper). In the case of $C_2H_5O_2$, this method was not applicable, because the absorption cross section of $C_2H_5O_2$ in the near infrared region is not well known. Therefore, the initial Cl-atom concentration was first quantified by transforming them into HO_2 radicals through their fast reaction with excess CH_3OH, which can reliably be quantified [18,[19]. Thereafter, CH_3OH was switched for C_2H_6, and it was supposed that the resulting peroxy radical concentration was equal to the HO_2 concentration. **Figure 5** shows typical experimental results for the reaction of $C_3H_7O_2$ with OH radicals.

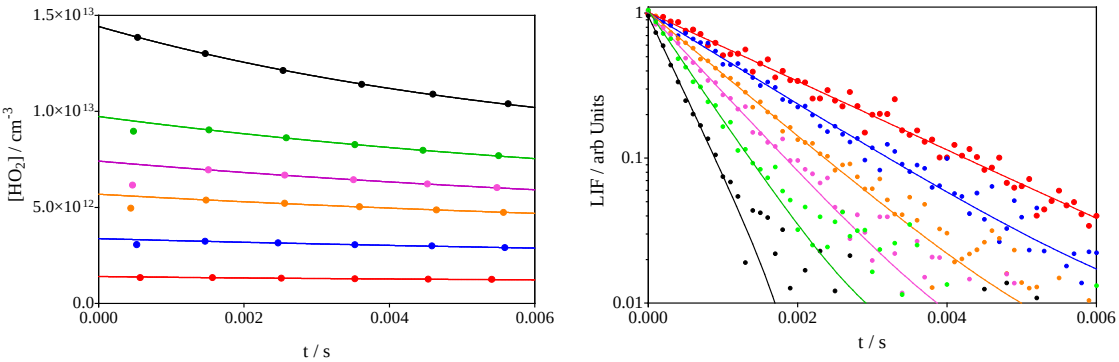

Figure 5: Left graph: HO_2 concentration time profiles used to quantify the initial Cl-atom concentration through exptrapolation of the decay to t=0: $[CH_3OH] = 2\times10^{14}$ cm^{-3}, $[O_2] = 2.7\times10^{17}$ cm^{-3}, $[(COCl)_2]$ increased from $(0.4 - 3.5)\times10^{14}$ cm^{-3}, from bottom to top. Right graph: OH decays for the reaction of $C_3H_7O_2$ with OH, *i.e.* same conditions as left graph, but replacing CH_3OH by $[C_3H_8] = 3.1\times10^{14}$ cm^{-3}. Figure adapted from Figure 1 in [15].

This way, a rate constant of k_{12} = (1.2±0.3)×10^{-10} cm^3s^{-1} was obtained, slightly faster than the rate constants of (R9). In a follow-up work, Assaf *et al*. [15] have also determined the rate constants for the two next-larger peroxy radicals, $C_3H_7O_2$ and $C_4H_9O_2$, with OH. Both radicals have been generated the same way as described above for $C_2H_5O_2$: the reaction of Cl-atoms with the corresponding hydrocarbon, with the Cl-atoms being quantified in back-to-back experiments with CH_3OH. Rate constants of (1.4±0.3)×10^{-10} cm^3s^{-1} and (1.5±0.3)×10^{-10} cm^3s^{-1} have been determined for propyl- and butylperoxy, respectively. All results are summarized in **Table 2**. Some test experiments were carried out using the photolysis of the corresponing alkyl iodides as precursor for the larger peroxy radicals, and again rate constants in the range of 3×10^{-10} cm^3s^{-1} have been found, supporting the hypothesis that the presence of I-atoms or accumulated I_2 molecules systematically biased the experiments of Bossolasco *et al*. [7].

Product yields and atmospheric implications

The reaction of RO_2 radicals with OH radicals might become competitive at decreasing NO concentrations. In the case of CH_3O_2, this will be the case in remote marine boundary layers, while the reaction of peroxy radicals generated from larger hydrocarbons might become competitive in remote biogenic environments. Therefore, it is interesting to determine the product yields for the reaction of larger peroxy radicals. A first theoretical investigation of the reaction of $C_2H_5O_2$ with OH radicals was carried out by Liu *et al*. [45], who determined the PES at the CCSD(T)/6-311++G(2df,2p)//B3LYP/6-311+G(d,p) level of theory. The results showed that, same as for CH_3O_2, the $C_2H_5O_2$ + OH reaction proceeds on both the singlet and the triplet PES. On the singlet PES, the favorable pathway is the addition of OH radical to the terminal oxygen atom of the $C_2H_5O_2$ radical, leading to the formation of trioxide $C_2H_5O_3H$ through a barrierless process. The trioxide then directly decomposes to the products C_2H_5O and HO_2 radicals. On the triplet PES, the predominant pathways are the abstraction of a hydrogen atom forming biradical products (CH_3CHO_2) and ($CH_2CH_2O_2$) with barriers of 12.02 and 19.19 kJ mol^{-1}, respectively. The properties of the trioxide $C_2H_5O_3H$ were investigated and the results indicate that the trioxide can exist stably in the atmosphere owing to a significantly large and negative enthalpy of formation (-118.44 kJ/mol).

The only experimental investigation of the product yields for the reaction of larger peroxy radicals with OH radicals was carried out by Assaf *et al*. [40]. Using the same technique as in the case of CH_3O_2 [35], *i.e*. the simultaneous quantitative detection of OH and HO_2 radicals by cw-CRDS, coupled to a simultaneous generation of OH and RO_2 radicals by 248nm photolysis of XeF_2 in presence of H_2O and different hydrocarbons, they determined the HO_2 yield for C_1 – C_4 peroxy radicals. It was found that at 50 Torr total pressure the HO_2 yield strongly decreased with increasing

size of the alkyl moiety of the peroxy radical: $\phi_{CH_3O_2}$ = (0.90±0.1), $\phi_{C_2H_5O_2}$ = (0.75±0.15), $\phi_{C_3H_7O_2}$ = (0.41±0.08), $\phi_{C_4H_9O_2}$ = (0.15±0.03). An accompanying theoretical study optimized the geometries and rovibrational characteristics of the critical points on the PES at the M06-2X/aug-*cc*pVTZ level of theory and further refined the relative energies at the CCSD(T)/aug-*cc*-pVTZ level of theory. RRKM master equation calculations could explain the clear decrease in HO_2 yield with increasing size of the alkyl moiety by an increased stabilization of the corresponding trioxide, ROOOH. Extrapolation of the experimental results to atmospheric conditions showed that the stabilized adduct, ROOOH, would be the nearly exclusive product of the reaction between OH radicals and peroxy radicals containing more than 3 C-atoms such as peroxy radicals obtained from the oxidation of biogenic hydrocarbons.

Table 2: Summary of rate constant and HO_2 yield measurements for the reaction of different RO_2 + OH radicals

Reaction	Precursor	k / cm^3s^{-1}	HO_2 yield / %	Reference
CH_3O_2 + OH	XeF_2 + CH_4 / H_2O	$(8.4\pm1.7)\times10^{-11}$ $(1.0\pm0.4)\times10^{-10}$	90 ±10	Yan *et al*. [13], Assaf *et al*. [14,[35], this work
$C_2H_5O_2$ + OH	XeF_2 + C_2H_6 / H_2O	$(1.2\pm0.3)\times10^{-10}$ $(1.3\pm0.3)\times10^{-10}$	75±15	Farago *et al*. [44] Assaf *et al*. [15,[40]
$C_3H_7O_2$ + OH	XeF_2 + n-C_3H_8 / H_2O	$(1.4\pm0.3)\times10^{-10}$	41±8	Assaf *et al*. [15,[40]
$C_4H_9O_2$ + OH	XeF_2 + n-C_4H_{10} / H_2O	$(1.5\pm0.3)\times10^{-10}$	15±3	Assaf *et al*. [15,[40]

It can thus be supposed, that ROOOH is formed in remote biogenic environments and non-negligible concentrations can possibly accumulate, depending on the lifetime of this class of species. In a recent work, Fittschen *et al*. [46] suggested that this class of species might be responsible for an unidentified interference in OH quantification in remote biogenic environments. Indeed, several field campaigns in such environments [47,[48,[49], all carried out by laser induced fluorescence after gas expansion (FAGE), have measured OH concentrations up to a factor of 10 higher than predicted by models. To explain such high OH concentrations, the oxidation mechanisms of biogenic VOCs, and especially of isoprene, have since been investigated in detail by theory *e.g.* [50,[51] and experiment *e.g.* [52,[53] in order to unravel unknown mechanism of OH-recycling in absence of NO and has been included in models since then [54]. And even though new OH recycling chemistry has been discovered, the impact on the steady-state OH concentration is not high enough to explain the large disagreement between measurements and models. W. Brune and coworkers [55] suspected interferences in FAGE measurements to be at least partially responsible for the high OH concentrations measured under remote biogenic conditions. They upgraded their FAGE instrument to unravel such interferences by mixing high concentrations of C_3H_6 or C_3F_6 into the airflow just before intake into the FAGE instrument. This way, all ambient OH would react away, and any remaining signal would be identified

as interference. This way, they observed strong interferences in OH measurements with their FAGE instrument [55,[56], with the intensity increasing with decreasing NO concentration. Other groups also found interferences using the same technique of pre-injection [57,[58,[59]. The decomposition of Criegee intermediates within the FAGE cell has been suspected to be at the origin of this interference [57], however other groups could not confirm this hypothesis [59]. Currently there is no consensus on the origin of this interference. Fittschen *et al.* [46] have recently shown that ROOOH, generated from the reaction of butylperoxy or isoprenehydroxyperoxy radicals with OH radicals, leads in their FAGE instrument to OH interference. However, the mechanism of this OH generation is currently not clear and might be due to heterogeneous decomposition of ROOOH within their FAGE cell. As all FAGE instruments have different designs, other FAGE instruments might behave differently and more work is needed to investigate if this class of species could explain the high OH concentrations observed in earlier field campaigns in remote forested areas.

In the recent attempt of designing the next generation of explicit mechanism, based on a combination of the Generator for Explicit Chemistry and Kinetics of Organics in the Atmosphere, GECKO-A [60], and the Master Chemical Mechanism, MCM [4], the reactions of RO_2 radicals with OH radicals are taken into account [61], and the next few years will probably bring more knowledge about this class of reactions through well-designed experiments.

Conclusion

The reaction of peroxy radicals with OH radicals as a possible reaction pathway for peroxy radicals in low NO environments has been ignored in atmospheric chemistry models until recently. Its possible role in clean atmospheres was evoked for the first time in 2009 by Archibald et al. [6], but it was only since Bossolasco *et al.* [7] measured for the first time in 2014 a rate constant for the simplest reaction CH_3O_2 + OH, that common interest in this class of reaction grew. The current manuscript summarizes the findings that have been achieved since then: rate constants have been measured for peroxy radicals up to C4, and some product yields for the simplest RO_2 radicals have also been measured. The role of the reaction of CH_3O_2 + OH over tropical oceans has already been included in models, the major product of this reaction is CH_3O + HO_2, and it is clear now that this reaction is not a source for atmospheric methanol. The possible role of the reactions of larger peroxy radicals with OH in remote biogenic environments however has not yet been investigated. The major product of this reaction is the trioxide, ROOOH, a new class of species that can accumulate to sizeable concentrations in remote environments. Their fate will probably attract some interest in the coming years.

Acknowledgement

The author thanks the French ANR agency under contract No. ANR-11-LabX-0005-01 CaPPA (Chemical and Physical Properties of the Atmosphere), the Région Hauts-de-France, the Ministère de l'Enseignement Supérieur et de la Recherche (CPER Climibio) and the European Fund for Regional Economic Development for continuous funding.

References

[1] J. J. Orlando, G. S. Tyndall, Chem. Soc. Rev. 41 (2012) 6294-6317.
[2] G. S. Tyndall, R. A. Cox, C. Granier, R. Lesclaux, G. K. Moortgat, M. J. Pilling, A. R. Ravishankara, T. J. Wallington, J. Geophys. Res. 106 (2001) 12157-12182.
[3] S. M. Saunders, M. E. Jenkin, R. G. Derwent, M. J. Pilling, Atmos. Environ. 31 (1997) 1249-1249.
[4] S. M. Saunders, M. E. Jenkin, R. G. Derwent, M. J. Pilling, Atmos. Chem. Phys. 3 (2003) 161-180.
[5] C. Bloss, V. Wagner, A. Bonzanini, M. E. Jenkin, K. Wirtz, M. Martin-Reviejo, M. J. Pilling, Atmos. Chem. Phys. 5 (2005) 623-639.
[6] A. T. Archibald, A. S. Petit, C. J. Percival, J. N. Harvey, D. E. Shallcross, Atmos. Sci. Lett. 10 (2009) 102-108.
[7] A. Bossolasco, E. P. Faragó, C. Schoemaecker, C. Fittschen, Chem. Phys. Lett. 593 (2014) 7-13.
[8] E. P. Faragó, B. Viskolcz, C. Schoemaecker, C. Fittschen, J. Phys. Chem. A 117 (2013) 12802-12811.
[9] A. Parker, C. Jain, C. Schoemaecker, C. Fittschen, React. Kinet. Catal. Lett. 96 (2009) 291-297.
[10] J. Thiebaud, A. Aluculesei, C. Fittschen, J. Chem. Phys. 126 (2007) 186101.
[11] C. Fittschen, L. K. Whalley, D. E. Heard, Environ. Sci. Technol. 118 (2014) 7700–7701.
[12] L. K. Whalley, K. L. Furneaux, A. Goddard, J. D. Lee, A. Mahajan, H. Oetjen, K. A. Read, N. Kaaden, L. J. Carpenter, A. C. Lewis, J. M. C. Plane, E. S. Saltzman, A. Wiedensohler, D. E. Heard, Atmos. Chem. Phys. 10 (2010) 1555-1576.
[13] C. Yan, S. Kocevska, L. N. Krasnoperov, J. Phys. Chem. A 120 (2016) 6111–6121.
[14] E. Assaf, B. Song, A. Tomas, C. Schoemaecker, C. Fittschen, J. Phys. Chem. A 120 (2016) 8923-8932.
[15] E. Assaf, S. Tanaka, Y. Kajii, C. Schoemaecker, C. Fittschen, Chem. Phys. Lett. 684 (2017) 245-249.
[16] M. B. Pushkarsky, S. J. Zalyubovsky, T. A. Miller, J. Chem. Phys. 112. (2000) 10695-10698.
[17] D. B. Atkinson, J. L. Spillman, J. Phys. Chem. A 106 (2002) 8891-8902.
[18] J. Thiebaud, S. Crunaire, C. Fittschen, J. Phys. Chem. A 111 (2007) 6959-6966.
[19] Y. Tang, G. S. Tyndall, J. J. Orlando, J. Phys. Chem. A 114 (2010) 369-378.
[20] L. Onel, A. Brennan, M. Gianella, G. Ronnie, A. Lawry Aguila, G. Hancock, L. Whalley, P. W. Seakins, G. A. D. Ritchie, D. E. Heard, Atmos. Meas. Tech. Discuss. 10 (2017) 4877-4894.
[21] E. Assaf, L. Liu, C. Schoemaecker, C. Fittschen, Journal of Quantitative Spectroscopy & Radiative Transfer 211 (2018) 107-114.
[22] E. Assaf, C. Schoemaecker, L. Vereecken, C. Fittschen, Phys. Chem. Chem. Phys. 20 (2018) 8707.

[23] S. H. Mousavipour, Z. Homayoon, J. Phys. Chem. A 115 (2011) 3291-3300.
[24] W. Tsang, R. F. Hampson, J. Phys. Chem. Ref. Data 15 (1986) 1087.
[25] E. Hassinen, J. Koskikallio, Acta Chemica Scandinavica Series a-Physical and Inorganic Chemistry 33 (1979) 625-630.
[26] J. Weaver, R. Shortridge, J. Meagher, J. Heicklen, Journal of Photochemistry 4 (1975) 109-120.
[27] M. J. Yee Quee, J. C. J. Thynne, Berichte der Bunsengesellschaft für physikalische Chemie 72 (1968) 211-217.
[28] M. J. Y. Quee, J. C. J. Thynne, Transactions of the Faraday Society 62 (1966) 3154-3161.
[29] P. Biggs, C. E. Canosa-Mas, J.-M. Fracheboud, D. E. Shallcross, R. P. Wayne, J. Chem. Soc., Faraday Trans. 93 (1997) 2481-2486.
[30] U. Meier, H. H. Grotheer, G. Riekert, T. Just, Berichte der Bunsengesellschaft für physikalische Chemie 89 (1985) 325-327.
[31] L. Onel, A. Brennan, M. Gianella, J. Hooper, N. Ng, G. Hancock, L. Whalley, P. W. Seakins, G. A. D. Ritchie, D. E. Heard, Atmos. Meas. Tech. to be submitted (2019).
[32] T. J. Dillon, M. E. Tucceri, J. N. Crowley, Chemphyschem 11 (2010) 4011-4018.
[33] T. J. Dillon, M. E. Tucceri, J. N. Crowley, Phys. Chem. Chem. Phys. 8 (2006) 5185-5198.
[34] J.-F. Müller, Z. Liu, V. S. Nguyen, T. Stavrakou, J. N. Harvey, J. Peeters, Nat. Commun. 7 (2016) 13213.
[35] E. Assaf, L. Sheps, L. Whalley, D. Heard, A. Tomas, C. Schoemaecker, C. Fittschen, Environ. Sci. Technol. 51 (2017) 2170-2177.
[36] D. J. Jacob, B. D. Field, Q. Li, D. R. Blake, J. de Gouw, C. Warneke, A. Hansel, A. Wisthaler, H. B. Singh, A. Guenther, J. Geophys. Res.-Atmos. 110 (2005) D08303.
[37] V. Ferracci, I. Heimann, N. L. Abraham, J. A. Pyle, A. T. Archibald, Atmos. Chem. Phys. 18 (2018) 7109-7129.
[38] L. Sheps, J. Phys. Chem. Lett. 4 (2013) 4201-4205.
[39] E. Assaf, C. Fittschen, J. Phys. Chem. A 120 (2016) 7051-7059.
[40] E. Assaf, C. Schoemaecker, L. Vereecken, C. Fittschen, Int. J. Chem. Kinet. 50 (2018) 670–680.
[41] R. L. Caravan, M. A. H. Khan, J. Zádor, L. Sheps, I. O. Antonov, B. Rotavera, K. Ramasesha, K. Au, M.-W. Chen, D. Rösch, D. L. Osborn, C. Fittschen, C. Schoemaecker, M. Duncianu, A. Grira, S. Dusanter, A. Tomas, C. J. Percival, D. E. Shallcross, C. A. Taatjes, Nat. Commun. 9 (2018) 4343.
[42] D. L. Osborn, P. Zou, H. Johnsen, C. C. Hayden, C. A. Taatjes, V. D. Knyazev, S. W. North, D. S. Peterka, M. Ahmed, S. R. Leone, Rev. Sci. Instrum. 79 (2008) 104103.
[43] J. M. Anglada, A. Solé, Phys. Chem. Chem. Phys. 20 (2018) 27406-27417.
[44] E. P. Faragó, C. Schoemaecker, B. Viskolcz, C. Fittschen, Chem. Phys. Lett. 619 (2015) 196-200.
[45] Y. Liu, L. Chen, D. Chen, W. Wang, F. Liu, W. Wang, Chemical Research in Chinese Universities 33 (2017) 623-630.
[46] C. Fittschen, M. Al Ajami, S. Batut, V. Ferracci, S. Archer-Nicholls, A. T. Archibald, C. Schoemaecker, Atmos. Chem. Phys. 19 (2019) 349-362.
[47] A. Hofzumahaus, F. Rohrer, K. Lu, B. Bohn, T. Brauers, C. C. Chang, H. Fuchs, F. Holland, K. Kita, Y. Kondo, X. Li, S. Lou, M. Shao, L. Zeng, A. Wahner, Y. Zhang, Science 324 (2009) 1702-1704.
[48] L. K. Whalley, P. M. Edwards, K. L. Furneaux, A. Goddard, T. Ingham, M. J. Evans, D. Stone, J. R. Hopkins, C. E. Jones, A. Karunaharan, J. D. Lee, A. C. Lewis, P. S. Monks, S. J. Moller, D. E. Heard, Atmos. Chem. Phys. 11 (2011) 7223-7233.
[49] J. Lelieveld, T. M. Butler, J. N. Crowley, T. J. Dillon, H. Fischer, L. Ganzeveld, H. Harder, M. G. Lawrence, M. Martinez, D. Taraborrelli, J. Williams, Nature 452 (2008) 737-740.
[50] J. Peeters, T. L. Nguyen, L. Vereecken, Phys. Chem. Chem. Phys. 11 (2009) 5935-5939.
[51] J. Peeters, T. L. Nguyen, J. Phys. Chem. A (2012).

[52] P. O. Wennberg, K. H. Bates, J. D. Crounse, L. G. Dodson, R. C. McVay, L. A. Mertens, T. B. Nguyen, E. Praske, R. H. Schwantes, M. D. Smarte, J. M. S. Clair, A. P. Teng, X. Zhang, J. H. Seinfeld, Chem. Rev. 118 (2018) 3337-3390.
[53] H. Fuchs, A. Hofzumahaus, F. Rohrer, B. Bohn, T. Brauers, H. P. Dorn, R. Haseler, F. Holland, M. Kaminski, X. Li, K. Lu, S. Nehr, R. Tillmann, R. Wegener, A. Wahner, Nature Geosci advance online publication (2013).
[54] M. E. Jenkin, J. C. Young, A. R. Rickard, Atmos. Chem. Phys. 15 (2015) 11433-11459.
[55] J. Mao, X. Ren, W. H. Brune, D. M. Van Duin, R. C. Cohen, J.-H. Park, A. H. Goldstein, F. Paulot, M. R. Beaver, J. D. Crounse, P. O. Wennberg, J. P. DiGangi, S. B. Henry, F. N. Keutsch, C. Park, G. W. Schade, G. M. Wolfe, J. A. Thornton, Atmos. Chem. Phys. - ACP 12 (2012) 8009-8020.
[56] P. A. Feiner, W. H. Brune, D. O. Miller, L. Zhang, R. C. Cohen, P. S. Romer, A. H. Goldstein, F. N. Keutsch, K. M. Skog, P. O. Wennberg, T. B. Nguyen, A. P. Teng, J. DeGouw, A. Koss, R. J. Wild, S. S. Brown, A. Guenther, E. Edgerton, K. Baumann, J. L. Fry, Journal of the Atmospheric Sciences 73 (2016) 4699-4710.
[57] A. Novelli, K. Hens, C. Tatum Ernest, M. Martinez, A. C. Nölscher, V. Sinha, P. Paasonen, T. Petäjä, M. Sipilä, T. Elste, C. Plass-Dülmer, G. J. Phillips, D. Kubistin, J. Williams, L. Vereecken, J. Lelieveld, H. Harder, Atmos. Chem. Phys. 17 (2017) 7807-7826.
[58] A. Novelli, K. Hens, C. T. Ernest, D. Kubistin, E. Regelin, T. Elste, C. Plass-Dulmer, M. Martinez, J. Lelieveld, H. Harder, Atmospheric Measurement Techniques 7 (2014) 3413-3430.
[59] P. Rickly, P. S. Stevens, Atmospheric Measurement Techniques 11 (2018) 1-16.
[60] B. Aumont, S. Szopa, S. Madronich, Atmos. Chem. Phys. 5 (2005) 2497-2517.
[61] M. E. Jenkin, R. Valorso, B. Aumont, A. R. Rickard, Atmos. Chem. Phys. Discuss. 2019 (2019) 1-46.